

Article

Deformation Effect on Water Transport through Nanotubes

Ferlin Robinson, Majid Shahbabaie and Daejoong Kim *

Department of Mechanical Engineering, Sogang University, 35 Baekbeom-ro, Mapo-gu, Seoul 121-742, Korea; ferlin@sogang.ac.kr (F.R.); m.shahbabaie@gmail.com (M.S.)

* Correspondence: daejoong@sogang.ac.kr

Received: 31 October 2019; Accepted: 18 November 2019; Published: 21 November 2019



Abstract: In this study, we used non-equilibrium molecular dynamics to study the transport of water through deformed (6,6) Carbon Nanotubes (CNTs) and Boron Nitride Nanotubes (BNNTs). The results were then compared with that of the perfect nanotubes. The main aim of this study was to get a better insight into the deformation effect on water transport through nanotubes rather than directly comparing the CNTs and BNNTs. As the diameters of both types of nanotubes differ from each other for the same chiral value, they are not directly comparable. We carried out our study on deformations such as screw distortion, XY-distortion, and Z-distortion. XY-distortion of value 2 shows a change from single-file water transport to near-Fickian diffusion. The XY-distortions of higher value shows a notable negative effect on water transport when their distortion values get larger. These suggest that the degree of deformation plays a crucial role in water transport through deformed nanotubes. The Z-distortion of 2 showed discontinuous single-file chain formation inside the nanotubes. Similar phenomena are observed in both nanotubes, irrespective of their type, while the magnitudes of their effects vary.

Keywords: non-equilibrium molecular dynamics; deformed carbon nanotubes; deformed boron nitride nanotubes; water transport; diffusion; Z-distortion; XY-distortion; screw distortion

1. Introduction

Nanotubes (NTs) are prominent structures in many applications. From water desalination to microelectronics, their areas of application are wide. Their application areas are even getting broad every day, as they hold a promising future due to their distinctive properties. The discovery of carbon nanotubes (CNTs) by Sumio Iijima [1] has revolutionized the nano world. Since its discovery, the field of nanotechnology has achieved greater heights. Rubio et al. [2] predicted boron nitride nanotubes (BNNTs) in 1994, and they were experimentally discovered in 1995, by Chopra et al. [3]. In 2001, Hummer et al. [4] found that water can pass through CNTs spontaneously, using molecular dynamics simulation. Since then, many studies were carried out, using perfect CNTs and BNNTs for water transport and desalination. But the studies carried out on the deformed nanotubes are limited. Different types of deformation occur in nanotubes. They could be twisted, compressed, elongated, or bent during application and manufacturing. They could also have defects such as Stone–Wales, point vacancies, interstitials, etc., during manufacturing. He et al. [5] studied the effects of deformation degree and about the location of deformation in the carbon nanotubes on water transport. Feng et al. [6] showed that the transport diffusion of helium gas through deformed carbon nanotubes with screw deformation did not have any effect, while the XY-distortion and Z-distortion showed that the effect on transport diffusion is significant with an increase in temperature and distortions values. Even though there were earlier studies carried out on the water transport phenomena through deformed carbon nanotubes, water transport through nanotubes that have a twist or XY-distortion and Z-distortion have

not been studied extensively yet. Therefore, in this work, we studied the effect of deformations such as screw distortion, XY-distortion, and Z-distortion on water transport through long CNTs and BNNTs.

The effect of deformation on water transport through nanotubes is also of great importance to many biological, ion-selective channels. The ionic conduction through single-walled carbon nanotubes can directly be compared to them. Ion-channels are formed from proteins [7]. CNT-based nanodevices with controllable functions are widely used to mimic transmembrane channels. These transmembrane channels can be used as substitutes for certain channel proteins. Model membranes are needed to examine their application as transmembrane channels. Two methods are widely used to simulate this bio-membrane system [8]. The first method is to embed the CNT as channel in-between graphite sheets as the membrane. The atoms are deleted at desired locations, in order to accommodate the tube [9–11]. The second method is the CNT-bundle system. In this method, packed CNTs serve both as channels and the membrane to separate the reservoirs [12,13]. In this study, we used the first method. This study about the effect of deformation can be of greater use for designing transmembrane channels.

2. Simulation Details

2.1. Computational Domain and Structures

Figure 1 shows the schematic of the molecular dynamics setup used in this study for CNT and BNNT. In this study, we used CNTs and BNNTs with chirality (6,6) and length 100 Å in all simulations. As the Z-distortion name suggests, the nanotube deformation is along the Z-direction; hence, a nanotube of length 100 Å gets distorted to 90, 110, and 120 Å for distortion values of 0.9, 1.1, and 1.2, respectively. To compare the effect of different deformations on water transport, at least one physical property has to be kept constrained. In this study, the length was kept constrained; hence, the Z-distortion nanotubes were modeled considerably long, and then they were truncated to have the length ~100 Å.

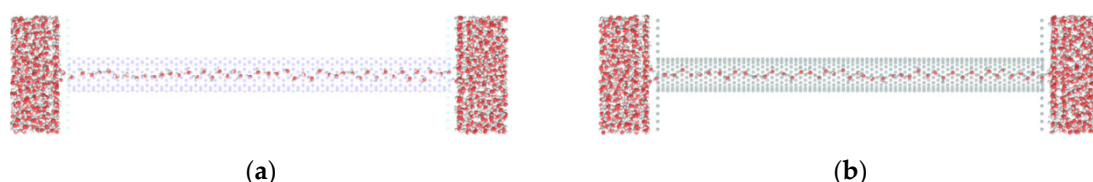


Figure 1. Schematic of molecular dynamics simulation setup: (a) boron nitride nanotube (BNNT) and (b) carbon nanotube (CNT).

The geometry of the perfect nanotube is shown in Figure 2a. The Z-distortion is induced in the perfect nanotube either by stretching or compressing along Z-axis, which increases or decreases the length of the nanotube, respectively. The stretch factor is given by Z'/Z_0 , where Z' is the total length after the perfect nanotube is distorted in the Z-direction [6]. The Z-distorted nanotube is shown in Figure 2b. The nanotube with the twist is shown in Figure 2c. The screw factors for the twisted nanotubes are given as β/Z_0 , where β is the twist angle and Z_0 is the length of the perfect nanotube. When an equal amount of force is applied in the positive and negative X or Y direction, XY-distorted carbon nanotubes can be obtained, as shown in Figure 2d. The XY-distorted nanotubes have an elliptical cross-section with ellipse factor $\Delta X/\Delta Y$.

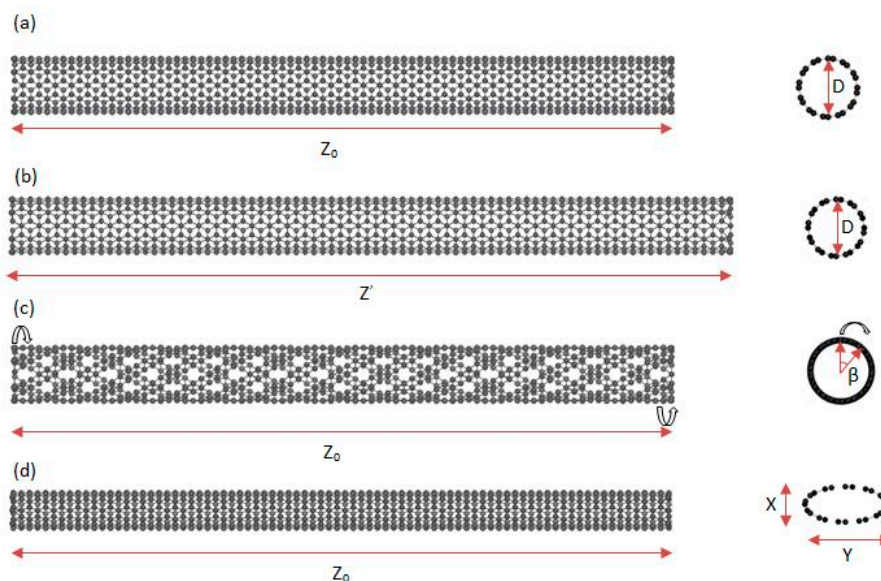


Figure 2. Perfect nanotube and different types of deformed nanotubes: (a) perfect nanotube; (b) Z-distortion nanotube (stretch factor: Z'/Z_0); (c) twisted nanotube (screw factor: β/Z_0); and (d) XY-distortion nanotube (ellipse factor: $e = \Delta X/\Delta Y$).

The perfect (6,6) CNT has a radius of 4.068 Å and bond length of 1.421 Å, whereas a perfect (6,6) BNNT has a radius of 4.211 Å and bond length of 1.47 Å. The description of the dimensions of the nanotubes is given in Table 1.

Table 1. Dimensions of different nanotubes used in this study. Z-distortion nanotube (stretch factor: Z'/Z_0), twisted nanotube (screw factor: β/Z_0), and XY-distortion nanotube (ellipse factor: $e = \Delta X/\Delta Y$).

Nanotube Type	Distortion Type	Major Axis Value (Å)	Minor Axis Value (Å)	Radius (Å)
CNT	Perfect NT	-	-	4.068
CNT	Screw Distortion 15	-	-	4.068
CNT	Screw Distortion 30	-	-	4.068
CNT	Screw Distortion 45	-	-	4.068
CNT	XY-distortion 2	10.560	6.277	-
CNT	XY-distortion 4	11.928	5.557	-
CNT	XY-distortion 6	12.331	5.376	-
CNT	Z-distortion 0.9	-	-	4.068
CNT	Z-distortion 1.1	-	-	4.068
CNT	Z-distortion 1.2	-	-	4.068
BNNT	Perfect NT	-	-	4.211
BNNT	Screw Distortion 15	-	-	4.211
BNNT	Screw Distortion 30	-	-	4.211
BNNT	Screw Distortion 45	-	-	4.211
BNNT	XY-distortion 2	11.217	6.494	-
BNNT	XY-distortion 4	12.599	5.749	-
BNNT	XY-distortion 6	13.008	5.561	-
BNNT	Z-distortion 0.9	-	-	4.211
BNNT	Z-distortion 1.1	-	-	4.211
BNNT	Z-distortion 1.2	-	-	4.211

2.2. Computational Methods

All molecular dynamics simulations were carried out by using the open-source software DL POLY 4.08 [14,15]. For visualization, VMD 1.9.4a12 software [16] was used. All simulations were carried out by using the non-equilibrium molecular dynamics (NEMD) method to derive the motion of the

molecules. LJ-potential is used to describe the interactions between the water molecules and the interaction between the CNT and water molecules. The LJ-potential is given by the following equation:

$$U(r_{ij}) = 4\epsilon[(\sigma/r_{ij})^{12} - (\sigma/r_{ij})^6]$$

where r_{ij} , σ , and ϵ are the interatomic bond vector, the balance distance where the interaction of particles is zero, and the depth of the potential well, respectively.

In this study, to model the flow, an external force field method is used. In this method, a constant force f is added to all water molecules along +Z direction to mimic the pressure-driven flow, whereas the pressure difference between the two sides of a membrane is as follows:

$$\Delta P = nf/A$$

where f is the applied force on each water molecule, n is the number of water molecules, and A is the membrane area. This is one of the widely accepted methods in molecular dynamics (MD) to simulate the pressure-driven flow [17]. Force is applied to the molecules, using the external force field known as the gravitational field in the DL POLY software, where the force is given by the following equation:

$$\underline{F} = m\underline{G}$$

where \underline{G} is the gravitational field which is given as input, \underline{F} is the force, and m is the mass of the water molecule.

All simulations were carried out with a gravitational field of 0.0185G applied to the molecules. The SPC/E water model used in this simulation has a contact angle $\theta = 95.3^\circ$ [18]. The LJ cross-interaction between the water molecules and carbon atoms are $\sigma_{C-O} = 0.319$ nm and $\epsilon_{C-O} = 0.392$ kJ/mol [18], which were determined by using the Lorentz-Berthelot mixing rules [19]. For water–water interactions, the default value of LJ parameter of SPC/E water model $\sigma_{O-O} = 0.3169$ nm and $\epsilon_{O-O} = 0.6498$ kJ/mol is used [20]. The LJ parameters of $\sigma_{B-O} = 0.331$ nm, $\epsilon_{B-O} = 0.5079$ kJ/mol, $\sigma_{N-O} = 0.326$ nm, and $\epsilon_{N-O} = 0.6276$ kJ/mol were used for the boron nitride interactions with water [21]. The bond lengths and angle degrees of the water molecule are constrained by SHAKE algorithm [22]. The canonical ensemble NVT is used for all the simulations, to update the velocity and position, along with Noosé-Hoover thermostat coupling, to maintain a constant temperature. A cut-off distance of 10 Å is used for LJ interactions.

3. Results and Analyses

A few key features were observed in the water transport phenomena through deformed nanotubes, including a change of single-file water chain transformation to two single-file water chains forming next to each other in the XY-distortion of 2 nanotubes, resembling a near-Fickian diffusion; formation of discontinuous single-file chain water transport in Z-distortion of 1.2 nanotubes; and a smattering water transport through XY-distortion of 4 and 6 nanotubes. Figure 3 shows the water transport through a perfect BNNT nanotube and the XY-distortion 2 BNNT nanotube.

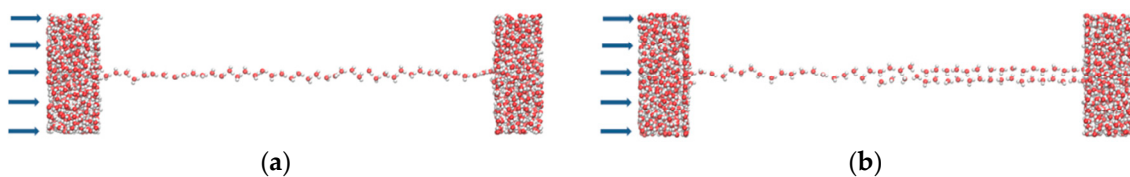


Figure 3. Visualization of water chain formed in-between two reservoirs: (a) perfect BNNT (b) BNNT with XY-distortion value 2.

3.1. Free Energy of Occupancy Fluctuations and Water Occupancy

Figure 4 shows the free energy of occupancy fluctuations as a function of the number of water molecules inside the nanotube for the CNT and BNNT with XY-distortion. The free energy of the occupancy fluctuations is calculated as follows:

$$\beta F(N) = -\ln p(N)$$

where $p(N)$ is the probability of finding exactly 'N' water molecules inside the nanotube, $F(N)$ is the free energy and $\beta = (k_B T)^{-1}$, k_B is the Boltzmann constant, and T is the temperature [4,23].

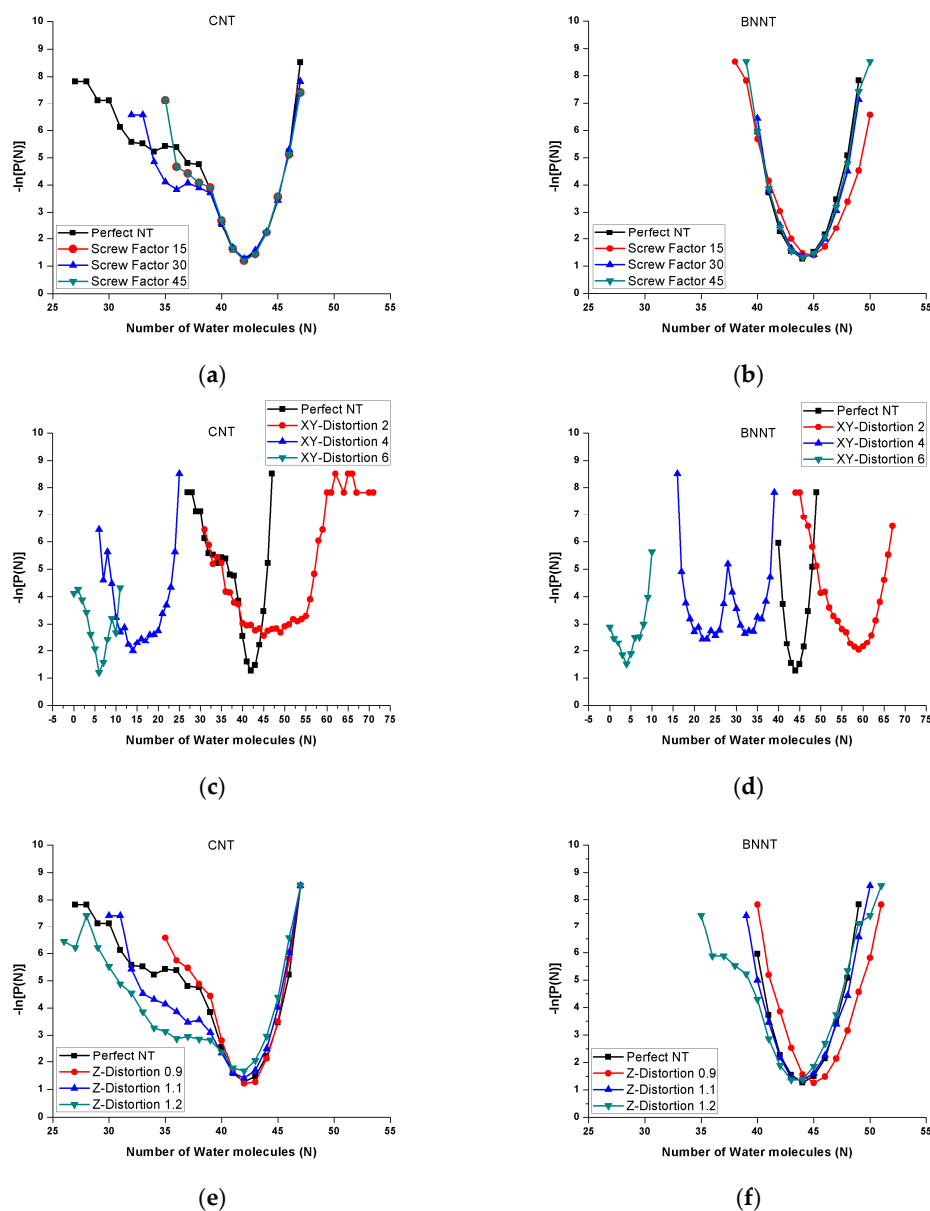


Figure 4. Free energy of occupancy fluctuation as a function of number of water molecules inside and different types of deformed nanotubes compared with perfect nanotubes: (a) carbon nanotube (CNT) with screw distortions; (b) boron nitride nanotube (BNNT) with screw distortions; (c) carbon nanotube (CNT) with XY-distortion; (d) boron nitride nanotube (BNNT) with XY-distortion; (e) carbon nanotube (CNT) with Z-distortion nanotube; and (f) boron nitride nanotube (BNNT) with Z-distortion.

The plot shows that the number of water molecules inside the perfect CNT ranges from 26 to 47. The most probable number of molecules is 42. The number of molecules inside the perfect BNNT ranges from 40 to 48. The most probable number is 44. It can be seen that the XY-distortion of 2 nanotubes accommodates the maximum number of water molecules when compared to others. The XY-distorted nanotubes of higher value show a significantly lower number of molecules in both the carbon and boron nitride nanotubes. The reason for the XY-distortion nanotubes to accommodate the maximum number of water molecules is that, when a nanotube is distorted in the XY-direction with the distortion value of 2, it has sufficient space to accommodate two water molecules side by side, as shown in Figure 3. Further increase in distortion value results in a higher energy barrier, higher friction, and decreased pore volume. This reduces water transport significantly.

Figure 5 shows the comparison of water occupancy of the CNTs and BNNTs with different deformations. For the BNNT with the XY-distortion of 4, even though it has a larger pore volume compared to the CNT of the same distortion, very few molecules enter the pore. This shows that the entrance effects play a major role in water flow through nanotubes. On the visualization of the simulation, using the VMD package, we found that, for the XY-distortion of 4 and 6 (CNT and BNNT), molecules entered the nanotube, but were unable to travel further continuously. This is due to the large friction and energy barrier inside these nanotubes. For these cases, only a handful of molecules were observed to travel through the pore from one end to the other. The screw-distorted nanotubes showed a negligible effect on the water transport phenomena. They behaved almost similarly to the perfect nanotubes. This can be observed from the water occupancy and free energy of occupancy fluctuation plots.

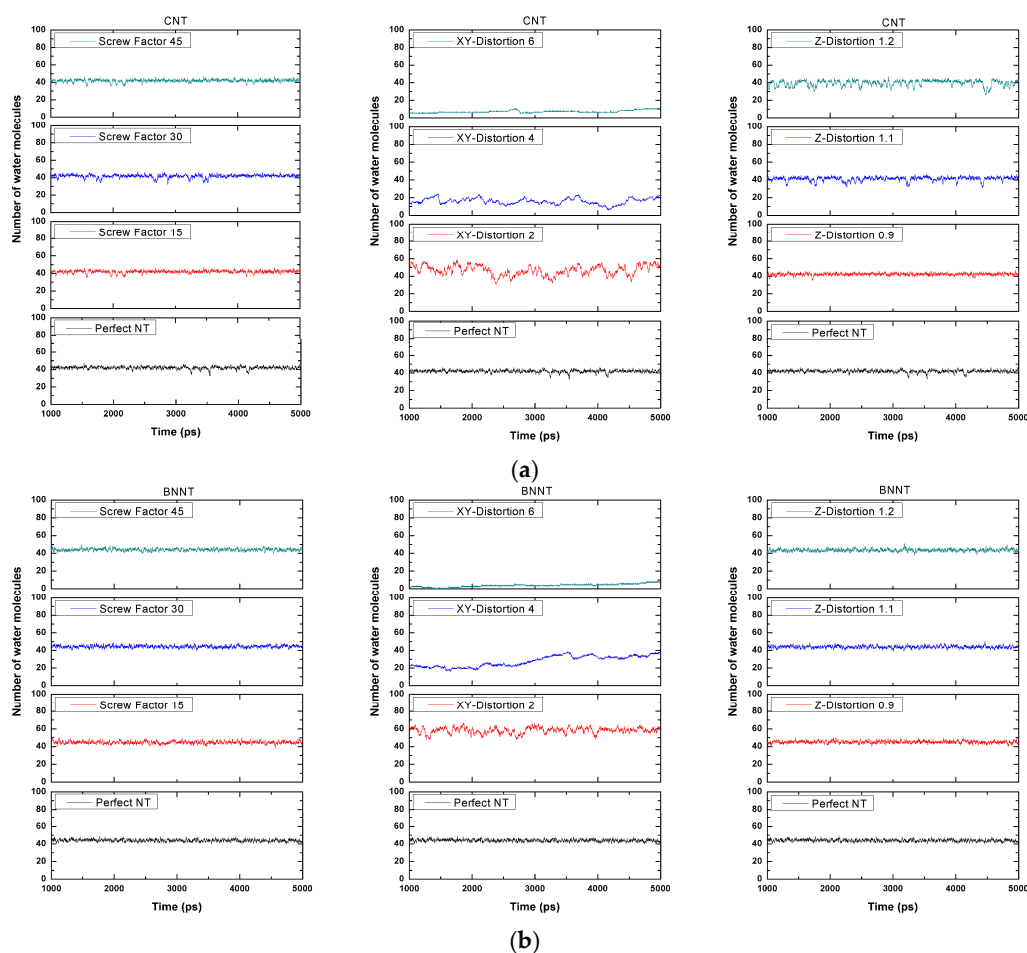


Figure 5. Water occupancy inside perfect and XY-distorted nanotubes versus time in picosecond: (a) carbon nanotube (CNT) and (b) boron nitride nanotube (BNNT).

3.2. Flux and Diffusion

Flux is created by the pressure that is applied to the water molecules inside the pool to push them through the nanotube. Water flux is calculated as the difference between the sum of the number of water molecules that move from the left side to the right side of the nanotube and the molecules which cross in the opposite direction [24]. Figure 6 shows the variation of flux based on different deformations.

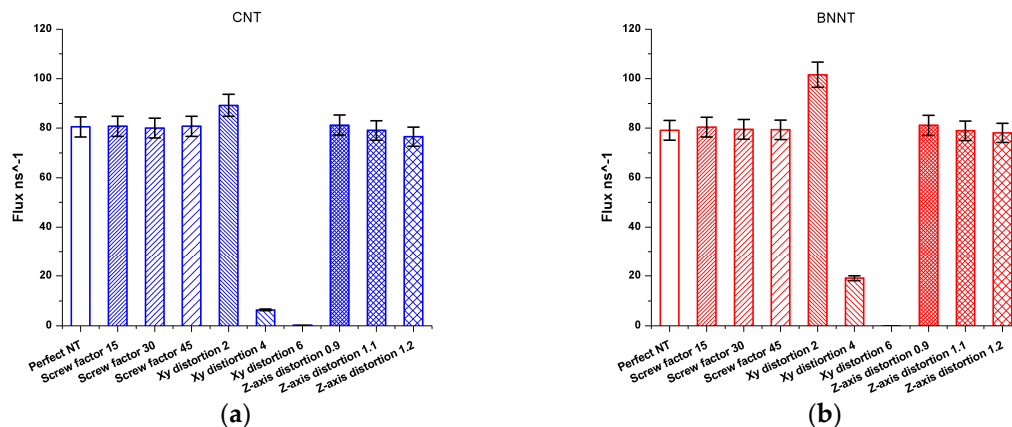


Figure 6. Variation of flux in perfect and different deformed nanotubes: (a) carbon nanotube (CNT) and (b) boron nitride nanotube (BNNT).

For both the carbon nanotube and boron nitride nanotube, the XY-distortion of 2 showed higher flux when compared to that of other nanotubes. XY-distortions of higher value showed much less flux when compared to the perfect nanotube. The number of molecules that cross the pore gradually decreases with an increase in the degree of deformation. The screw distorted nanotubes did not show any variations; they behave almost similarly to that of the perfect nanotube.

The diffusion coefficient of water through the nanotube is the measure of the mass of the water that diffuses through a unit surface of the nanotube in a unit time at a concentration gradient of unity. The axial diffusion coefficient of water molecules can be computed from the mean squared displacement (MSD). The MSD of the water molecule's center of mass can be calculated by using the relation used by Barati Farimani et al. [25]:

$$\langle |(\mathbf{r}(t) - \mathbf{r}(0))|^2 \rangle = ADt^n$$

where 'r' denotes the center of the mass coordinate of the water molecule. The angle bracket used in the equation defines the average over all the water molecules; 't' denotes the time interval; 'D' denotes the diffusion coefficient; 'A' denotes the dimensional factor values of 2, 4, and 6 for 1-, 2-, and 3-dimensional diffusion, respectively; and 'n' defines the type of the diffusion mechanism. The value of 'n' can be 0.5, 1, and 2, depending on how the MSD varies with time. These values of 'n' represent Single-File diffusion, Fickian diffusion, and ballistic diffusion, respectively. MSD of all the molecules in that direction with A = 2 is used to compute the average axial diffusion coefficient in Z-direction. In this simulation, the single-file diffusion is observed in all cases other than the XY-distorted nanotubes. In the XY-distorted nanotube of distortion value 2, a change from single-file to near-Fickian diffusion is observed. Hence, there is a significant increase in diffusion and flux.

Figure 7 shows the variation of diffusion coefficient for nanotubes with different types of deformation. The XY-deformation of 2 shows a relatively higher diffusion coefficient due to the increase in the pore volume of the nanotube when compared to other XY-distortions of higher value. This is in good agreement with the Hilder et al. [26] and Corry et al. [27]. It can be seen that there are significant values for diffusion for XY-distortions of 4 and 6 when compared with that of the flux. This is due to

the filling of water molecules near the entrance and exit of the nanotube, while the number of water molecules that completely travel from one end to the other is very low.

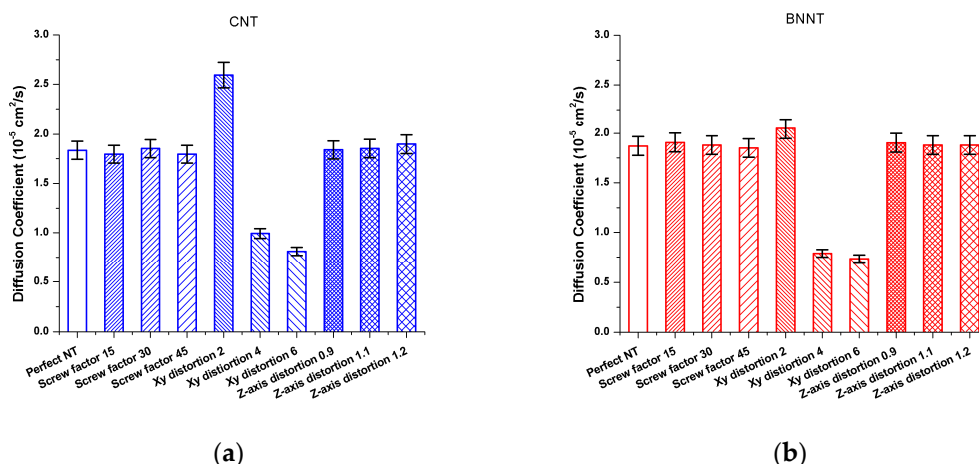


Figure 7. Pressure dependence of diffusion coefficient in perfect and different types of deformed nanotubes: (a) carbon nanotube (CNT) and (b) boron nitride nanotube (BNNT).

3.3. The Hydrogen Bonding

The average number of hydrogen bonds per water molecule inside the nanotube for the nanotubes with different deformations is given in the figure below for both BNNT and CNT.

We know that the number of hydrogen bonds that occurs inside the nanotube is a function of the length and the pore size. From Figure 8, we can observe that there is no significant increase in the number of hydrogen bonds formed inside the pore for the nanotubes, which has a twist, as they have the same length and pore size of that of the perfect nanotube. We observed that the nanotubes with the XY-distortion of 2 show a significantly higher value of hydrogen bonding per water molecule inside the nanotube when compared to others. This is due to the increase in the pore volume of the elliptical cross section of the nanotubes, which facilitates the accommodation of water molecules side by side inside the pore. Usually, a single-file water transport is observed in nanotubes in (6,6) nanotubes, but when they are distorted in XY-direction, it has sufficient space to accommodate two water molecules side by side, as shown clearly in the Figure 3.

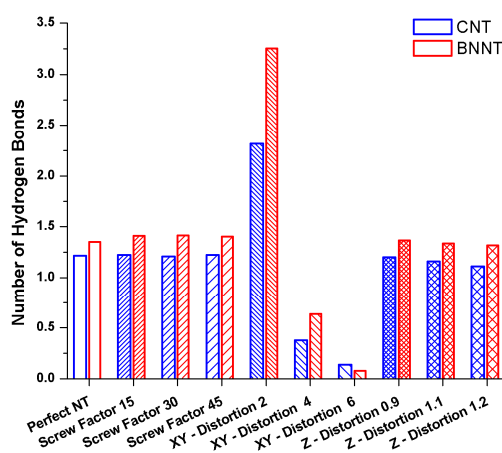


Figure 8. Average number of hydrogen bonds per water molecule formation inside the pore for perfect and different types of deformed nanotubes: carbon nanotubes (CNT) and boron nitride nanotubes (BNNT).

For both the CNT and BNNT, we can see a significant increase in the hydrogen bond, which decreases the mobility and formation of the more-bonded system. When compared between the diffusion and the number of hydrogen bond plots for the XY-distortion of 2, we can see that the diffusion in the CNT is higher with a lower hydrogen bond when compared with the BNNT. This shows that the formation of a more-bonded system decreases the water diffusion through the nanotubes. This is in good agreement with the results obtained by Mendonca et al. [28]. This facilitates the change of diffusion from single file transport to near-Fickian diffusion. The XY-distortion of 4 and 6 shows the accumulation of molecules near the entrance and exit of the pore. Due to the large energy barrier inside the pore and large interaction of the water molecules with the wall, the molecules can neither occupy the whole pore volume nor transport through them easily.

The Z-distortion of 1.2 of the nanotubes shows a noticeable decrease in the number of hydrogen bonds per water molecule when compared to other Z-distortions due to the stop-start diffusion of molecules near the entrance of the nanotube, as shown in the Figure 9. Even though this phenomenon is observed in both the CNT and BNNT, this phenomenon is predominant in the CNT when compared with that of the BNNT. To further understand this discontinuous flow phenomenon, the friction force, radial distribution function (RDF), and potential of mean force are studied for this particular case in detail for the CNT.

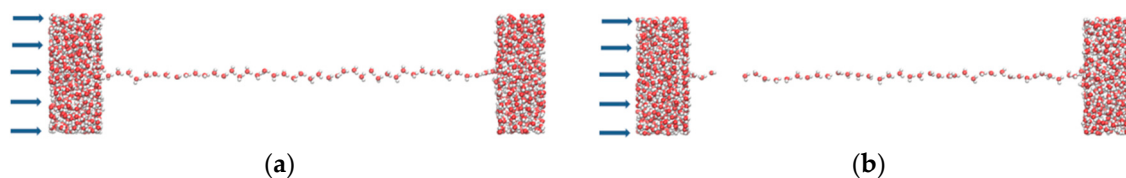


Figure 9. Visualization of water chain formed in-between two reservoirs: (a) perfect CNT and (b) CNT with Z-distortion value 1.2.

3.4. Friction Force and Trajectory

Discontinuous single-file diffusion is found in the CNT with the Z-distortion of 1.2, as shown in Figure 9. To investigate this phenomenon, the friction force is calculated. The friction force plays a significant role in water transport through the nanotubes. The friction force is large when there is a large interaction of water molecules with the nanotube walls.

Friction force is calculated by using the method suggested by Falk et al. [29]:

$$f(r) = dU(r) / dr = 24 (\epsilon/\sigma) [(\sigma/r)^7 - (\sigma/r)^{13}]$$

where 'r' is the distance between the oxygen atom of the water molecule and the nanotube wall atoms. Figure 10a shows the plot of friction force along the nanotube length for the carbon nanotube with Z-distortion of 1.2 and the perfect nanotube. It can be seen that the Z-distortion of 1.2 shows a higher friction force when compared to the perfect nanotube. This implies that there is less interaction between the walls of the perfect nanotube with the water molecules when compared to that of the Z-distortion of 1.2.

The discontinuity of the single-file water transport arises near the entrance of the nanotube. It is either followed by breakage of the single-file transport into short chains of molecules or filled up again at a faster pace. The molecules that follow after the broken single-file chain move relatively faster when compared to that of other molecules inside the nanotube. This can be viewed in Figure 10b, which shows the plot of the trajectory of a single molecule inside the perfect CNT compared to that of the CNT with Z-distortion of 1.2.

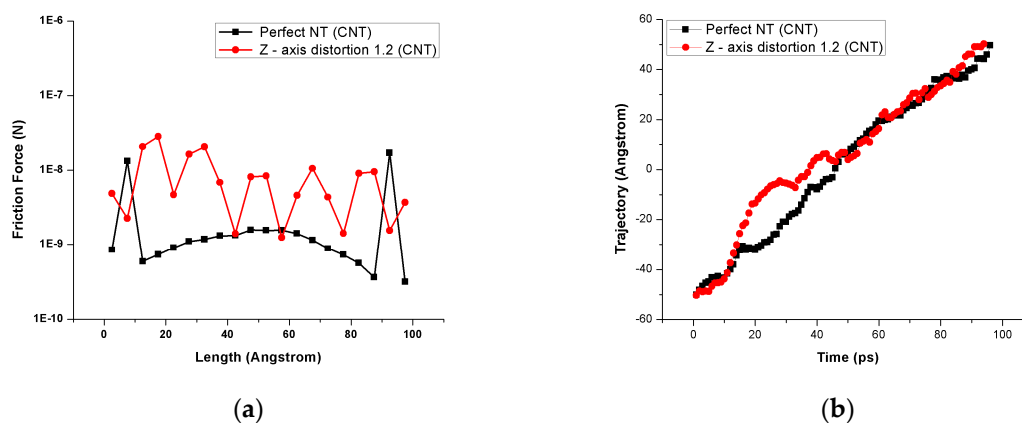


Figure 10. (a) Friction force inside the perfect nanotube and Z-distortion 1.2 CNT. (b) Comparison of water molecule trajectory inside perfect CNT and CNT with Z-distortion value 1.2.

3.5. Radial Distribution Function and Potential of Mean Force

The structural change of water molecules in the simulation cell can be described by the radial distribution function. Radial distribution function describes the atomic density variation as a function of distance from a particular atom [29]. Figure 11a illustrates the radial distribution function (RDF) of water molecules inside perfect and the Z-distortion 1.2 carbon nanotube.

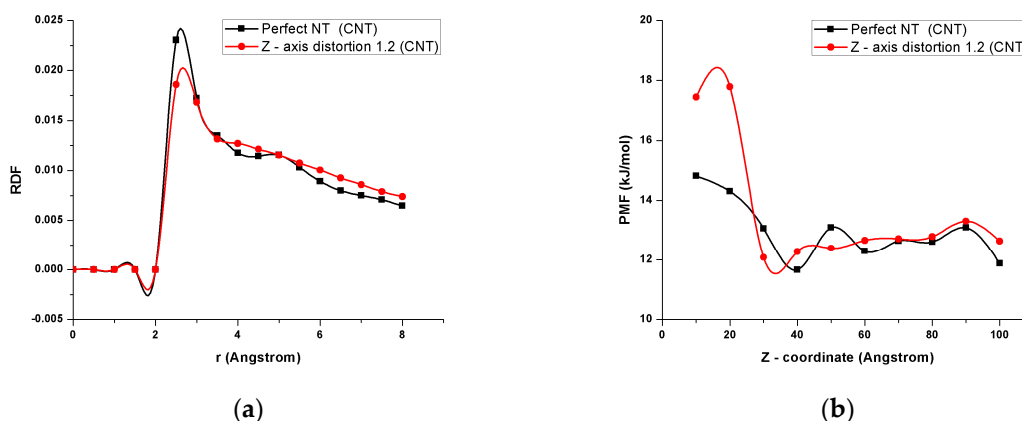


Figure 11. (a) Radial distribution function of water molecules within the perfect carbon nanotube and carbon nanotube with Z-distortion 1.2. (b) Potential of mean force within the perfect carbon nanotube and carbon nanotube with Z-distortion 1.2.

The Z-distortion of 1.2 shows the more favorable interplay between the water and walls of the nanotube. It shows that the density increases in the vicinity of the Z-distortion of 1.2 carbon nanotube walls when compared to that of the perfect carbon nanotube walls. Therefore, this strong interplay between the oxygen atom of the water molecules and the Z-distortion of 1.2 carbon nanotube walls reduces the transport rate of water inside this nanotube. When compared to that of the Z-distortion of the 1.2 carbon nanotube, perfect carbon nanotubes show less interplay between the oxygen atoms of the water molecule with the walls of the nanotube. Thus, it favors faster water transport when compared to the Z-distortion of 1.2.

Potential of mean force (PMF) calculations inside the nanotubes help to understand the amount of energy barrier that exists inside the nanotube [30]. Water molecules have to overcome this energy barrier to move through the nanotube. The potential of mean force is calculated as follows:

$$\text{PMF} = (-k_{\text{B}}T) \ln g(x)$$

where $g(x)$ is the radial distribution function (RDF), k_{B} the Boltzmann constant, and T the thermodynamic temperature [16]. Figure 11b shows that the potential of mean force inside the Z-distortion of 1.2 CNT is significantly larger than the perfect CNT, so the water molecules should have larger energy to conduct through the nanopore. This result further supports the reason for the discontinuous flow occurring inside the Z-distortion of the 1.2 carbon nanotube.

4. Conclusions

In conclusion, we have investigated the different types of deformations such, as screw distortion, XY-distortion, and Z-distortion in both carbon nanotubes and boron nitride nanotubes of 100 Å in length with chirality (6,6).

The effects of these deformations on both the nanotubes (BNNT and CNT) are quite similar. The formation of the more bonded system due to the increase in hydrogen bonds inside the nanotube decreases the diffusion of water through them. This is similar to the results reported by Mendonca et al. [28]. As Feng et al. [6] reported for the diffusion of helium gas through deformed nanotubes, the screw distortion did not have any significant impact on water transport, but the impact of the XY-distortion and Z-distortion were quite significant. The XY-deformation of higher value had a compelling negative effect on water transport, while the XY-distorted nanotubes of value 2 showed encouraging effects on water transport through the nanotubes. These results point to the importance of nanotube structure on water transport phenomena.

Further studies could be carried out for the XY-distortion of values less than 2 and for values slightly higher than 2 for optimizing the value which supports better water transport. These studies can also help to design better transmembrane channels and other relative nanodevices.

Author Contributions: Conceptualization, F.R.; methodology, F.R.; software, F.R.; validation, F.R., M.S. and D.K.; formal analysis, F.R.; investigation, D.K. and M.S.; resources, D.K.; data curation, F.R.; writing—original draft preparation, F.R.; writing—review and editing, M.S. and D.K.; visualization, F.R.; supervision, D.K. and M.S.; project administration, D.K. and M.S.; funding acquisition, D.K.

Funding: This research received no external funding.

Conflicts of Interest: The authors declare no conflict of interest.

References

1. Iijima, S. Helical microtubules of graphitic carbon. *Nature* **1991**, *354*, 56–58. [\[CrossRef\]](#)
2. Rubio, A.; Corkill, J.L.; Cohen, M.L. Theory of graphitic boron nitride nanotubes. *Phys. Rev. B* **1994**, *49*, 5081–5084. [\[CrossRef\]](#)
3. Chopra, N.G.; Luyken, R.J.; Cherrey, K.; Crespi, V.H.; Cohen, M.L.; Louie, S.G.; Zettl, A. Boron Nitride Nanotubes. *Science* **1995**, *269*, 966. [\[CrossRef\]](#)
4. Hummer, G.; Rasaiah, J.C.; Noworyta, J.P. Water conduction through the hydrophobic channel of a carbon nanotube. *Nature* **2001**, *414*, 188–190. [\[CrossRef\]](#)
5. He, J.-X.; Lu, H.-J.; Liu, Y.; Wu, F.-M.; Nie, X.-C.; Zhou, X.-Y.; Chen, Y.-Y. Asymmetry of the water flux induced by the deformation of a nanotube. *Chin. Phys. B* **2012**, *21*, 054703. [\[CrossRef\]](#)
6. Feng, J.; Chen, P.; Zheng, D.; Zhong, W. Transport diffusion in deformed carbon nanotubes. *Phys. A Stat. Mech. Appl.* **2018**, *493*, 155–161. [\[CrossRef\]](#)
7. Amiri, H.; Shepard, K.L.; Nuckolls, C.; Hernández Sánchez, R. Single-Walled Carbon Nanotubes: Mimics of Biological Ion Channels. *Nano Lett.* **2017**, *17*, 1204–1211. [\[CrossRef\]](#) [\[PubMed\]](#)
8. Liu, B.; Li, X.; Li, B.; Xu, B.; Zhao, Y. Carbon Nanotube Based Artificial Water Channel Protein: Membrane Perturbation and Water Transportation. *Nano Lett.* **2009**, *9*, 1386–1394. [\[CrossRef\]](#) [\[PubMed\]](#)
9. Gong, X.; Li, J.; Lu, H.; Wan, R.; Li, J.; Hu, J.; Fang, H. A charge-driven molecular water pump. *Nat. Nanotechnol.* **2007**, *2*, 709–712. [\[CrossRef\]](#) [\[PubMed\]](#)

10. Wan, R.; Li, J.; Lu, H.; Fang, H. Controllable Water Channel Gating of Nanometer Dimensions. *J. Am. Chem. Soc.* **2005**, *127*, 7166–7170. [[CrossRef](#)] [[PubMed](#)]
11. Li, J.; Gong, X.; Lu, H.; Li, D.; Fang, H.; Zhou, R. Electrostatic gating of a nanometer water channel. *Proc. Natl. Acad. Sci. USA* **2007**, *104*, 3687–3692. [[CrossRef](#)] [[PubMed](#)]
12. Kalra, A.; Garde, S.; Hummer, G. Osmotic water transport through carbon nanotube membranes. *Proc. Natl. Acad. Sci. USA* **2003**, *100*, 10175–10180. [[CrossRef](#)] [[PubMed](#)]
13. Zhu, F.; Schulten, K. Water and Proton Conduction through Carbon Nanotubes as Models for Biological Channels. *Biophys. J.* **2003**, *85*, 236–244. [[CrossRef](#)]
14. Todorov, I.T.; Smith, W.; Trachenko, K.; Dove, M.T. DL_POLY_3: New dimensions in molecular dynamics simulations via massive parallelism. *J. Mater. Chem.* **2006**, *16*, 1911–1918. [[CrossRef](#)]
15. Bush, I.J.; Todorov, I.T.; Smith, W. A DAFT DL_POLY11URL distributed memory adaptation of the Smoothed Particle Mesh Ewald method. *Comput. Phys. Commun.* **2006**, *175*, 323–329. [[CrossRef](#)]
16. Humphrey, W.; Dalke, A.; Schulten, K. VMD: Visual molecular dynamics. *J. Mol. Graph.* **1996**, *14*, 33–38. [[CrossRef](#)]
17. Zhu, F.; Tajkhorshid, E.; Schulten, K. Theory and simulation of water permeation in aquaporin-1. *Biophys. J.* **2004**, *86*, 50–57. [[CrossRef](#)]
18. Werder, T.; Walther, J.H.; Jaffe, R.L.; Halicioglu, T.; Koumoutsakos, P. On the Water–Carbon Interaction for Use in Molecular Dynamics Simulations of Graphite and Carbon Nanotubes. *J. Phys. Chem. B* **2003**, *107*, 1345–1352. [[CrossRef](#)]
19. Raghunathan, A.V.; Park, J.H.; Aluru, N.R. Interatomic potential-based semiclassical theory for Lennard-Jones fluids. *J. Chem. Phys.* **2007**, *127*, 174701. [[CrossRef](#)]
20. Tang, D.; Li, L.; Shahbabaie, M.; Yoo, Y.-E.; Kim, D. Molecular Dynamics Simulation of the Effect of Angle Variation on Water Permeability through Hourglass-Shaped Nanopores. *Materials* **2015**, *8*, 7257–7268. [[CrossRef](#)]
21. Won, C.Y.; Aluru, N.R. Water Permeation through a Subnanometer Boron Nitride Nanotube. *J. Am. Chem. Soc.* **2007**, *129*, 2748–2749. [[CrossRef](#)] [[PubMed](#)]
22. Ryckaert, J.-P.; Ciccotti, G.; Berendsen, H.J.C. Numerical integration of the cartesian equations of motion of a system with constraints: Molecular dynamics of n-alkanes. *J. Comput. Phys.* **1977**, *23*, 327–341. [[CrossRef](#)]
23. Shahbabaie, M.; Kim, D. Molecular Dynamics Simulation of Water Transport Mechanisms through Nanoporous Boron Nitride and Graphene Multilayers. *J. Phys. Chem. B* **2017**, *121*, 4137–4144. [[CrossRef](#)] [[PubMed](#)]
24. Shahbabaie, M.; Kim, D. Effect of hourglass-shaped nanopore length on osmotic water transport. *Chem. Phys.* **2016**, *477*, 24–31. [[CrossRef](#)]
25. Barati Farimani, A.; Aluru, N.R. Spatial Diffusion of Water in Carbon Nanotubes: From Fickian to Ballistic Motion. *J. Phys. Chem. B* **2011**, *115*, 12145–12149. [[CrossRef](#)] [[PubMed](#)]
26. Hilder, T.A.; Gordon, D.; Chung, S.-H. Salt Rejection and Water Transport Through Boron Nitride Nanotubes. *Small* **2009**, *5*, 2183–2190. [[CrossRef](#)]
27. Corry, B. Designing Carbon Nanotube Membranes for Efficient Water Desalination. *J. Phys. Chem. B* **2008**, *112*, 1427–1434. [[CrossRef](#)]
28. Mendonça, B.H.S.; de Freitas, D.N.; Köhler, M.H.; Batista, R.J.C.; Barbosa, M.C.; de Oliveira, A.B. Diffusion behaviour of water confined in deformed carbon nanotubes. *Phys. A Stat. Mech. Appl.* **2019**, *517*, 491–498. [[CrossRef](#)]
29. Falk, K.; Sedlmeier, F.; Joly, L.; Netz, R.R.; Bocquet, L. Ultralow Liquid/Solid Friction in Carbon Nanotubes: Comprehensive Theory for Alcohols, Alkanes, OMCTS, and Water. *Langmuir* **2012**, *28*, 14261–14272. [[CrossRef](#)]
30. Won, C.Y.; Joseph, S.; Aluru, N.R. Effect of quantum partial charges on the structure and dynamics of water in single-walled carbon nanotubes. *J. Chem. Phys.* **2006**, *125*, 114701. [[CrossRef](#)]

